

# CODIMENSION TWO UMBILIC POINTS ON SURFACES IMMERSED IN $\mathbb{R}^3$

RONALDO GARCIA AND JORGE SOTOMAYOR

ABSTRACT. In this paper is studied the behavior of lines of curvature near umbilic points that appear generically on surfaces depending on two parameters.

## 1. INTRODUCTION

The study of principal curvature lines, along which surfaces immersed in  $\mathbb{R}^3$  bend maximally and minimally, goes back to the work of Monge [13]. There was determined the behavior of principal lines on the triaxial ellipsoids. The analysis around umbilic points, at which surfaces bend equally in all directions, had a preponderant role in this work, which may be regarded as the first one on the subject of foliations with singularities.

In 1896 Darboux [3] carried out a complete local analysis of umbilic points in the class of analytic surfaces, under generic conditions on the third derivatives of the immersions of surfaces at the umbilic points. Darboux established that there are three generic patterns, called here *Darbouxian Umbilics*  $D_1$ ,  $D_2$  and  $D_3$ , illustrated in Fig. 1. This figure represents both families of principal curvature lines, minimal  $\mathcal{F}_1$  and maximal  $\mathcal{F}_2$ , associated to minimal and maximal principal curvatures  $k_1$  and  $k_2$ ,  $k_1 < k_2$ , expect at umbilic points. The subscript stands for the number of umbilic separatrices approaching the point. In this case the number is the same for both the minimal and maximal principal curvature foliations.

This result of Darboux was rediscovered by Gutierrez and Sotomayor, [7, 8] in the context of Structural Stability of principal lines on surfaces of class  $C^4$ ,  $r \geq 4$ . They showed that the Darbouxian umbilic points are generic, corroborating in  $C^4$ ,  $r \geq 4$ , the above mentioned results of Darboux, and characterize the structurally stable ones, under small  $C^3$  deformations of the surface. See also the work of Bruce and Fidal [2]. In Sotomayor [15] can be found comments on the early developments on lines of curvature and their relation with recent works on foliations with singularities geometrically defined on surfaces immersed in  $\mathbb{R}^3$ .

---

*Key words and phrases.* umbilic point, principal curvature lines.  
MSC: 53C12, 34D30, 53A05, 37C75.

Both authors are fellows of CNPq. This work was done under the project CNPq PADCT 620029/2004-8 and CNPq 473824/04-3. The first author was partially supported by FUNAPE/UFG.

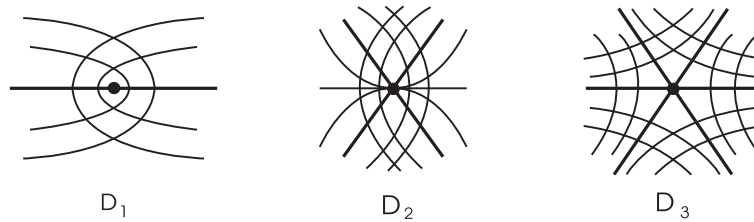


FIGURE 1. Principal curvature lines near the Darbouxian  $D_i$ ,  $i = 1, 2, 3$ , umbilic points and their separatrices

In [4, 9] the simplest bifurcation patterns of Darbouxian umbilics were established by Garcia, Gutierrez and Sotomayor. This corresponds to the weakening of the Darbouxian structural stability conditions in the most stable and generic way, leading to *codimension one umbilic points* and their generic bifurcations. See section 2 for a review of the analytic expressions of these conditions.

The expression *codimension one* means that the umbilic points appear generically on one-parameter families of immersed surfaces. This corresponds to families in general position with respect to a regular part of the bifurcation set –a hypersurface– in the infinite dimensional space of immersions. The two patterns of umbilics of codimension one established in [4, 9], denominated  $D_2^1$  and  $D_{2,3}^1$ , are illustrated in Fig. 2. The superscript stands for the codimension and the subscripts stand for the number of separatrices approaching the umbilic point. In the first case, the number of separatrices is the same for both the minimal and maximal principal curvature foliations. In the second case, they are not equal and, in our notation, appear separated by a comma. See Theorem 2 in section 2.

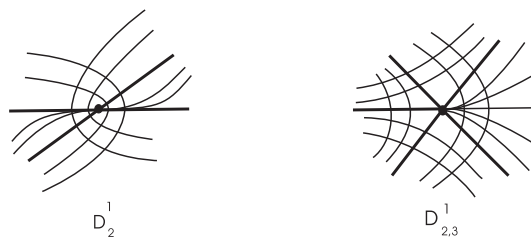


FIGURE 2. Lines of Curvature near Codimension one Umbilic Points  $D_2^1$ , left, and  $D_{2,3}^1$ , right.

This paper pursues the analysis in [4], increasing in one unity the number of parameters on which the immersion of the surface depends. The general *codimension two* umbilic points exhibited by generic bi-parametric families of surfaces immersed in  $\mathbb{R}^3$ , consisting on four patterns – called  $D_1^2$ ,  $D_{2p}^2$ ,  $D_3^2$  and  $D_{2h}^2$  *codimension two* umbilic points – will be established here. The superscript stands for the codimension. The symbols  $p$ , for *parabolic*, and  $h$ ,

for *hyperbolic*, have been added to the subscripts above in order to distinguish types that are not discriminated only by the number of separatrices.

The first three patterns can be described as follows:  $D_1^2$  is topologically equivalent to a point  $D_1$ ;  $D_{2p}^2$  is topologically equivalent to a point  $D_2$ ;  $D_3^2$  is topologically equivalent to a point  $D_3$ . See Fig. 1.

The pattern  $D_{2h}^2$  is illustrated in Fig. 3, where  $c$  and  $B$  are coefficients defined in equation (1), pertinent to a Monge presentation of the immersion at the umbilic point. This pattern is new with respect to previous types. Also no proof of its structure has been found in the literature.

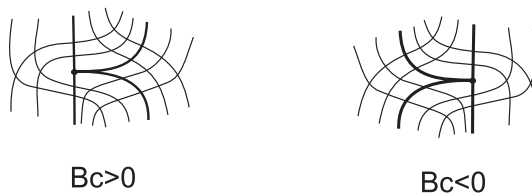


FIGURE 3. Lines of curvature near the umbilic point  $D_{2h}^2$

Section 2 is devoted to review some background on umbilic points of codimension less than two. The local configurations of principal lines at umbilic points of types  $D_1^2$ ,  $D_{2p}^2$ ,  $D_3^2$  and  $D_{2h}^2$  are established in Section 3. The fact that these points actually are those of *codimension two*, in a geometric sense, is established in Section 4.

The study of the bifurcation diagrams of lines of principal curvature lines at umbilic points for bi-parametric families of surfaces in  $\mathbb{R}^3$ , roughly prepared in Section 4, involve some technical and lengthy work, especially in the case of  $D_{2h}^2$ , and will be postponed to a future paper [5].

## 2. PRELIMINARIES ON UMBILIC POINTS

The following assumptions will hold from now on.

Let  $p_0$  be an umbilic point of an immersion  $\alpha$  of an oriented surface  $\mathbb{M}$  into  $\mathbb{R}^3$ , with a once for all fixed orientation. It will be assumed that  $\alpha$  is of class  $C^k$ ,  $k \geq 6$ . In a local Monge chart near  $p_0$  and a positive adapted 3-frame,  $\alpha$  is given by  $\alpha(u, v) = (u, v, h(u, v))$ , where

$$\begin{aligned}
 h(u, v) = & \frac{k}{2}(u^2 + v^2) + \frac{a}{6}u^3 + \frac{b}{2}uv^2 + \frac{c}{6}v^3 + \frac{A}{24}u^4 + \frac{B}{6}u^3v \\
 & + \frac{C}{4}u^2v^2 + \frac{D}{6}uv^3 + \frac{E}{24}v^4 + \frac{a_{50}}{120}u^5 + \frac{a_{41}}{24}u^4v \\
 & + \frac{a_{32}}{12}u^3v^2 + \frac{a_{23}}{12}u^2v^3 + \frac{a_{14}}{24}uv^4 + \frac{a_{05}}{120}v^5 + h.o.t
 \end{aligned} \tag{1}$$

Notice that, without loss of generality, the term  $u^2v$  has been eliminated from this expression by means of a rotation in the  $(u, v)$ -frame.

According to [16] and [17], the differential equation of lines of curvature in terms of  $I = Edu^2 + 2Fdudv + Gdv^2$  and  $II = edu^2 + 2fdudv + gdv^2$  around  $p_0$  is:

$$(Fg - Gf)dv^2 + (Eg - Ge)dudv + (Ef - Fe)du^2 = 0. \quad (2)$$

Therefore the functions  $L = Fg - Gf$ ,  $M = Eg - Ge$  and  $N = Ef - Fe$  are:

$$\begin{aligned} L &= h_u h_v h_{vv} - (1 + h_v^2) h_{uv} \\ M &= (1 + h_u^2) h_{vv} - (1 + h_v^2) h_{uu} \\ N &= (1 + h_u^2) h_{uv} - h_u h_v h_{uu}. \end{aligned}$$

Extensive calculation gives

$$\begin{aligned} L &= -bv - \frac{1}{2}Bu^2 - (C - k^3)uv - \frac{1}{2}Dv^2 - \frac{a_{41}}{6}u^3 \\ &\quad + \frac{1}{2}(4bk^2 + k^2a - a_{32})u^2v + \frac{1}{2}(3k^2c - a_{23})uv^2 - \frac{1}{6}(a_{14} + 3bk^2)v^3 + h.o.t \\ M &= (b - a)u + cv + \frac{1}{2}(C - A + 2k^3)u^2 + (D - B)uv + \frac{1}{2}(E - C - 2k^3)v^2 \\ &\quad + \frac{1}{6}[6bk^2(a + b) + a_{32} - a_{50}]u^3 + \frac{1}{2}(a_{23} + 2ck^2 - a_{41})u^2v \\ &\quad + \frac{1}{2}[a_{14} - a_{32} - 2k^2(a + b)]uv^2 + \frac{1}{6}(a_{05} - a_{23} - 6ck^2)v^3 + h.o.t \\ N &= bv + \frac{1}{2}Bu^2 + (C - k^3)uv + \frac{1}{2}Dv^2 + \frac{1}{6}a_{41}u^3 \\ &\quad + \frac{1}{2}(a_{32} - 3ak^2)u^2v + \frac{1}{2}(a_{23} - k^2c)uv^2 + \frac{1}{6}(a_{14} - 3bk^2)v^3 + h.o.t \end{aligned} \quad (3)$$

These expressions appear, up to order two, in Darboux [3], including also the coefficient of  $u^2v$ , annihilated here by a rotation in the frame  $(u, v)$ .

**2.1. Darbouxian Umbilic Points.** For the sake of completeness we will state now the result of Gutierrez and Sotomayor in [7, 8] about the local behavior of curvature lines near a Darbouxian umbilic point.

**Theorem 1.** Let  $p_0$  be an umbilic point and consider the Monge chart as in equation (1).

Suppose that the transversality condition:

$$T) \quad b(b - a) \neq 0$$

and one the following –Darbouxian– conditions holds.

$$D_1) \quad \left(\frac{c}{2b}\right)^2 - \frac{a}{b} + 2 < 0$$

$$D_2) \quad \left(\frac{c}{2b}\right)^2 + 2 > \frac{a}{b} > 1, \quad a \neq 2b$$

$$D_3) \quad \frac{a}{b} < 1$$

Then the behavior of lines of curvature near the umbilic point, separated in two principal foliations  $\mathcal{F}_1$  and  $\mathcal{F}_2$ , with a common singularity at  $p_0$  is as illustrated in Fig. 1.

The local configuration near umbilics is explained in terms of the phase portraits of the singularities of the Lie-Cartan vector field suspension,  $X_{\mathcal{F}}$ , of the implicit differential equation  $\mathcal{F}(u, v, p) = 0$ , where,

$$\begin{aligned} \mathcal{F}(u, v, p) &= Lp^2 + Mp + N = 0, \quad p = \frac{dv}{du} \\ X_{\mathcal{F}} &= (\mathcal{F}_p, p\mathcal{F}_p, -(\mathcal{F}_u + p\mathcal{F}_v)). \end{aligned} \tag{4}$$

The projection by  $\pi(u, v, p) = (u, v)$  of the integral curves of  $X_{\mathcal{F}}$ , restricted to  $\mathcal{F}(u, v, p) = 0$  are the lines of curvature near the umbilic point. The singularities of  $X_{\mathcal{F}}$ , restricted to the invariant regular surface  $\mathcal{F}(u, v, p) = 0$ , are given by  $(0, 0, p_i)$  where  $p_i$  is a root of the equation  $(\mathcal{F}_u + p\mathcal{F}_v)(0, 0, p) = p(bp^2 - cp + a - 2b) = 0$ . In in the present Darbouxian case, these singularities are hyperbolic saddles and nodes.

In Fig. 4 is illustrated the behavior of  $X_{\mathcal{F}}$  in each of the Darbouxian cases. Here only one of the principal foliations has been drawn, for the sake of simplicity. The other one is the projection of the other half cylinder, not sketched in the Figure.

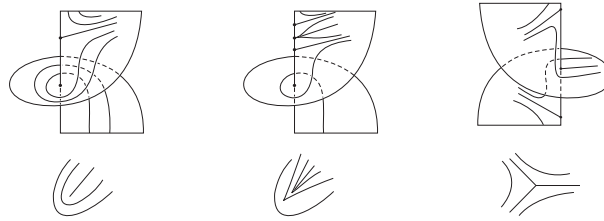


FIGURE 4. Lie-Cartan Suspension of the  $D_i$  umbilic points

**Remark 1.** *With reference to the illustrations in Fig. 1 of principal curvature foliations, arises the question of deciding which foliation is minimal and which one is maximal.*

*The procedure to follow, going back to the basic definitions, is to evaluate the normal curvature function  $k_n(p_0, [du : dv]) = II(p_0, [du : dv])/I(p_0, [du : dv])$ , on the surface  $\mathcal{F}(p_0, [du : dv]) = 0$ . Locally, near the projective line  $\mathcal{P} = \{(0, 0, p)\}$  the set  $\mathcal{F}^{-1}(0) \setminus \mathcal{P}$  has two open connected components defined by  $\mathcal{C}_1 = \{(p_0, [du : dv]) : k_n(p_0, [du : dv]) = k_1(p_0)\} \setminus \mathcal{P}$  and  $\mathcal{C}_2 = \{(p_0, [du : dv]) : k_n(p_0, [du : dv]) = k_2(p_0)\} \setminus \mathcal{P}$ . The projection of the phase portrait of  $X_{\mathcal{F}}$  in the component  $\mathcal{C}_1$  (resp.  $\mathcal{C}_2$ ) defines the minimal (resp. maximal) principal foliation.*

*This procedure applies to all isolated umbilics and will not be repeated for those studied below.*

**2.2. Codimension One Umbilic Points.** For future reference, we review a basic result of [4, 9] for umbilics in generic families of surfaces depending on one parameter.

**Theorem 2.** [4, 9] Let  $p_0$  be an umbilic point and consider  $\alpha(u, v) = (u, v, h(u, v))$  as in equation (1). Suppose the following conditions hold:

$$\begin{aligned} D_2^1 & \quad cb(b-a) \neq 0 \text{ and either } \left(\frac{c}{2b}\right)^2 - \frac{a}{b} + 1 = 0 \quad \text{or} \quad a = 2b. \\ D_{2,3}^1 & \quad b = a \neq 0 \quad \text{and} \quad \chi = cB - (C - A + 2k^3)b \neq 0. \end{aligned}$$

Then the behavior of lines of curvature near the umbilic point  $p_0$  in cases  $D_2^1$  and  $D_{2,3}^1$ , is as illustrated in Fig. 2.

In Fig. 5 is illustrated the behavior of  $X_{\mathcal{F}}$  in each of the semi Darbouxian cases.

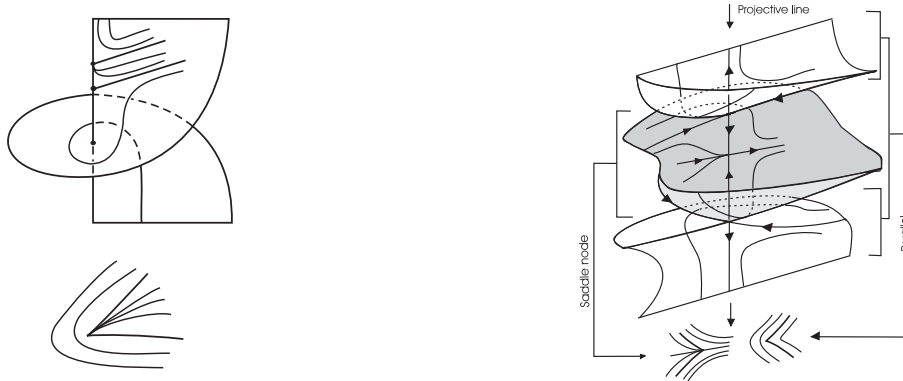


FIGURE 5. Lie-Cartan suspension  $D_2^1$ , left, and  $D_{2,3}^1$ , right.

In this section, umbilic points which appear generically and stably on one-parameter families of surfaces have been described in terms of hyperbolic and partially hyperbolic singularities of vector fields. The analogy between the structurally stable plane vector field singularities and stable umbilic points on surfaces is complete in the Darbouxian case. In the  $D_2^1$  and  $D_{2,3}^1$ , codimension one umbilics, the analogy is only partial. The full analysis depends both on the classic saddle-node, in the plane, and on the phase portrait of a singularity of a vector field on a conic Morse critical point on the surface  $\mathcal{F}^{-1}(0)$ .

### 3. PATTERNS OF CODIMENSION TWO UMBILIC POINTS

In this section will be studied the four simplest umbilic points, denominated  $D_1^2$ ,  $D_{2p}^2$ ,  $D_3^2$  and  $D_{2h}^2$ , not discussed previously, assuming that the non-degeneracy conditions imposed in Theorem 2 of section 2, are violated in the mildest possible fashion and are substituted by suitable higher order hypotheses. This procedure goes back to the notions of *higher order stability* due to Andronov and Leontovich [1]. See also [4] and [6]. Here, referring to equation 1,  $j^3h(0)$  does not vanish and the hypotheses are expressed in terms of  $j^4h(0)$  and  $j^5h(0)$ .

### 3.1. $D_1^2$ Umbilic Points.

**Proposition 1.** *Let  $p_0$  be an umbilic point and  $\alpha(u, v) = (u, v, h(u, v))$  as in equation 1.*

*If  $D_1^2$ ):  $c = 0$  and  $a = 2b \neq 0$ , then the configuration of principal lines near  $p_0$  is topologically equivalent to that of a Darbouxian  $D_1$  umbilic point. See Fig. 1, left.*

*Proof.* The differential equation of curvature lines is given by equation (4), where, for the present case:

$$\begin{aligned} L &= -bv - \frac{1}{2}Bu^2 + (k^3 - C)uv - \frac{1}{2}Dv^2 + h.o.t \\ M &= -bu + \frac{1}{2}(2k^3 - A + C)u^2 + (D - B)uv + \frac{1}{2}(E - 2k^3 - C)v^2 + h.o.t \\ N &= bv + \frac{1}{2}Bu^2 + (-k^3 + C)uv + \frac{1}{2}Dv^2 + h.o.t \end{aligned}$$

Direct calculation shows that  $\mathcal{F}_v(0, 0, 0) = b \neq 0$ . The solution,  $v = v(u, p)$  of the implicit equation  $\mathcal{F}(u, v(u, p), p) = 0$  near  $(0, 0, 0)$  is given by:

$$v(u, p) = up - \frac{B}{2b}u^2 + O(3)$$

Near the origin, in the chart  $(u, p)$ , the vector field  $X_{\mathcal{F}}$  is given by

$$\begin{aligned} \dot{u} &= \mathcal{F}_p(u, v(u, p), p) = -bu + O(2) \\ \dot{p} &= -(\mathcal{F}_u + p\mathcal{F}_v)(u, v(u, p), p) = u[-B + O(1)] + bp^3. \end{aligned}$$

Therefore the point 0 is a topological saddle of order three, having the projective line as the unique center manifold.

The analysis of  $X_{\mathcal{F}}$  outside a neighborhood of the  $(0, 0, 0)$  is trivial, since the three singular points on the  $p$ -axis are concentrated at the origin. In the chart  $(u, v, q)$ ,  $q = du/dv$ , the correspondent Lie-Cartan vector field is regular at  $(0, 0, 0)$ . Therefore, gluing the phase portraits as in Darbouxian  $D_1$  umbilic point, the result follows. See Fig. 4, left.  $\square$

### 3.2. $D_{2p}^2$ and $D_3^2$ Umbilic Points.

**Proposition 2.** *Let  $p_0$  be an umbilic point and  $\alpha(u, v) = (u, v, h(u, v))$  be as in equation 1.*

*If  $a = b \neq 0$ ,  $\chi = cB - b(C - A + 2k^3) = 0$  and  $\xi = 12k^2b^3 + (a_{32} - a_{50})b^2 + (3B^2 - 3BD - ca_{41})b + 3cB(C - k^3) \neq 0$ , then the principal configurations of lines of curvature fall into one of the two cases:*

- i) *Case  $D_{2p}^2$ :  $\xi b < 0$ , which is topologically a  $D_2$  umbilic and*
- ii) *Case  $D_3^2$ :  $\xi b > 0$ , which is topologically a  $D_3$  umbilic.*

*See Fig. 1, center and right, respectively.*

*Proof.* The differential equation of curvature lines is given by  $\mathcal{F}(u, v, p) = Lp^2 + Mp + N = 0$ ,  $p = \frac{dv}{du}$  where the coefficients are given from equation 3 as follows:

$$\begin{aligned}
L &= -bv - \frac{1}{2}Bu^2 - (C - k^3)uv - \frac{1}{2}Dv^2 - \frac{1}{6}a_{41}u^3 + \frac{1}{2}(5bk^2 - a_{32})u^2v \\
&\quad + \frac{1}{2}(3k^2c - a_{23})uv^2 - \frac{1}{6}(a_{14} + 3bk^2)v^3 + h.o.t \\
M &= cv + \frac{1}{2}(C - A + 2k^3)u^2 + (D - B)uv + \frac{1}{2}(E - C - 2k^3)v^2 \\
&\quad + \frac{1}{6}[12bk^2 + a_{32} - a_{50}]u^3 + \frac{1}{2}(a_{23} + 2ck^2 - a_{41})u^2v \\
&\quad + \frac{1}{2}[a_{14} - a_{32} - 4k^2b]uv^2 + \frac{1}{6}(a_{05} - a_{23} - 6ck^2)v^3 + h.o.t \\
N &= bv + \frac{1}{2}Bu^2 + (C - k^3)uv + \frac{1}{2}Dv^2 + \frac{1}{6}a_{41}u^3 + \frac{1}{2}(a_{32} - 3bk^2)u^2v \\
&\quad + \frac{1}{2}(a_{23} - k^2c)uv^2 + \frac{1}{6}(a_{14} - 3bk^2)v^3 + h.o.t
\end{aligned} \tag{5}$$

Direct calculation shows that  $\mathcal{F}_v(0, 0, 0) = b \neq 0$ . The solution  $v = v(u, p)$  of equation  $\mathcal{F}(u, v(u, p), p) = 0$  is given by:

$$v(u, p) = -\frac{B}{2b}u^2 + \left[\frac{3B(C - k^3) - a_{41}b}{6b^2}\right]u^3 + \left[\frac{cB - (C - A + 2k^3)b}{2b^2}\right]u^2p + O(4)$$

Therefore, in the chart  $(u, p)$ , the Lie-Cartan vector field  $X_{\mathcal{F}}$  is given by

$$\begin{aligned}
\dot{u} &= \mathcal{F}_p(u, v(u, p), p) \\
\dot{p} &= -(\mathcal{F}_u + p\mathcal{F}_v)(u, v(u, p), p),
\end{aligned}$$

which amounts to

$$\begin{aligned}
\dot{u} &= -\frac{\chi}{2b}u^2 + \frac{\xi}{6b^2}u^3 + \frac{c\chi}{2b^2}u^2p + O(4) \\
\dot{p} &= -Bu - bp + O(2),
\end{aligned} \tag{6}$$

where  $\xi = 12k^2b^3 + (a_{32} - a_{50})b^2 + (3B^2 - 3BD - ca_{41})b + 3cB(C - k^3)$ .

As  $\chi = cB - b(C - A + 2k^3) = 0$ , the singular point 0 is a topological saddle of order three when  $b\xi > 0$  and is a topological node when  $b\xi < 0$ .

The other singular points of the vector field  $X_{\mathcal{F}} = (\mathcal{F}_p, p\mathcal{F}_p, -(\mathcal{F}_u + p\mathcal{F}_v))$  are  $(0, 0, p_1)$  and  $(0, 0, p_2)$ , where  $p_i$  are the roots of the equation  $bp^2 - cp - b = 0$ , which are topological saddles. In fact,

$$DX_{\mathcal{F}}(0, 0, p_i) = \begin{bmatrix} 0 & -2bp_i + c & 0 \\ 0 & p_i(2bp_i - c) & 0 \\ b_1 & b_2 & 3bp_i^2 - 2cp_i - b \end{bmatrix},$$



where  $b_1 = 2Bp_i^2 - 2p_iC - p_ik^3 + p_iA - B - p_i^3k^3 + p_i^3C - Dp_i^2$  and  $b_2 = p_i^2k^3 + 2p_i^2C - 2p_iD + p_iB - C + k^3 + Dp_i^3 - p_i^2E$

The non zero eigenvalues of  $DX_{\mathcal{F}}(0, 0, p_i)$  are  $\lambda_1 = -2bp_i^2 + cp_i = -(cp_i + 2b) = -b(p_i^2 + 1)$  and  $\lambda_2 = 3bp_i^2 - 2cp_i - b = cp_i + 2b = b(p_i^2 + 1)$ .

The implicit surface  $\mathcal{F}(u, v, p) = 0$  has two critical points, one at  $(0, 0, p_1)$  and the other at  $(0, 0, p_2)$ . They are of Morse conic type if and only if  $\chi \neq 0$ . Otherwise, they have quadratic co-rank 1 and Morse index 1.

Below it will be established that, at these points, the surface is locally a topological disk. This will follow from the smooth right equivalence of  $\mathcal{F}$  with  $x^2 - y^2 + z^3 = 0$ , provided  $\xi \neq 0$ . The smoothness class ( $\geq 1$ ) is explained below as a consequence of [11].

In fact, at the points  $p_1$  and  $p_2$ , the Hessian of  $\mathcal{F}$  is given by:

$$Hess(\mathcal{F}(0, 0, p_i)) = \begin{bmatrix} 0 & b_{12} & 0 \\ b_{12} & -\frac{p_i(cB - Eb + Dc + Ab)}{b} & c - 2bp_i \\ 0 & c - 2bp_i & 0 \end{bmatrix}$$

where  $b_{12} = \frac{p_i}{b} ((k^3 - C)c + (D - B)b)$ .

The eigenvalues of  $Hess(\mathcal{F}(0, 0, p_i))$  are  $0 < \mu_1, \mu_2 < 0$ , with  $\mu_1\mu_2 = -[b_{12}^2 + (c - 2bp_i)^2] < 0$ , and  $\mu_3 = 0$ . The eigenspace associated to  $\mu_3 = 0$  is spanned by  $\ell_3 = ((2bp_i - c)b, 0, p_i((k^3 - C)c + (D - B)b))$ .

Consider the implicit equation

$$(\mathcal{F}_v(u, v, p_i + q), \mathcal{F}_p(u, v, p_i + q)) = (0, 0).$$

By the Implicit Function Theorem, the solution of the equation above is a regular curve  $c$ . A regular parametrization of  $c$  is given by

$$c(s) = (b(2bp_i - c)s, 0(2), p_i + p_i[(k^3 - C)c + (D - B)b]s + 0(2)).$$

Therefore,  $\gamma(s) = \mathcal{F}(c(s))$  is such that  $\gamma(0) = p_i$ ,  $\gamma'(0) = 0$ ,  $\gamma''(0) = -p_ib(c^2 + 4b^2)\chi = 0$  and  $\gamma'''(0) = p_i(2bp_i - c)^3\xi \neq 0$ . This follows from the fact that  $p_i$  are solutions of  $bp^2 - cp + b = 0$ .

The calculation leading to the expression for  $\gamma'''(0)$ , linear in  $\xi$ , has been corroborated by Computer Algebra.

Therefore, by the Generalized Morse Lemma – see Thom [18], pp. 75, and Lopez de Medrano [11]– there exist coordinates  $(u_1, v_1, w_1)$  such that  $\mathcal{F}(u_1, v_1, w_1) = \mu_1u_1^2 + \mu_2v_1^2 + w_1^3$ .

Direct examination of proof in this paper gives that the coordinates are of smoothness class  $k - 2 - 3 \geq 1$ ,  $k - 2$  in the class of  $\mathcal{F}$ .

The phase portrait of  $X_{\mathcal{F}}$  near the singular point  $(0, 0, p_i)$  is shown in Fig. 6.

This picture illustrates the orientation reversing projection of the surface into the plane, which occurs in  $D_3^2$ . To get the orientation preserving case it suffices to look at this picture upside down.

To conclude the proof it must be noticed that for  $X_{\mathcal{F}}$  the singular point 0 is a node when  $b\xi < 0$  and it is a saddle when  $b\xi > 0$ , which follows from

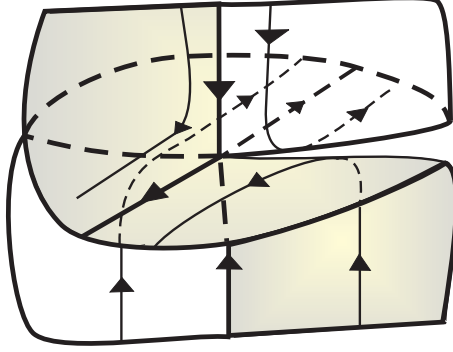


FIGURE 6. Phase portrait of  $X_{\mathcal{F}}$  in a neighborhood of a critical point of corank 1.

equation (6), while  $p_i$  ( $i = 1, 2$ ) are always saddles. This leads to  $D_{2p}^2$  in the first case and to  $D_3^2$  in the second case.  $\square$

### 3.3. $D_{2h}^2$ Umbilic Points.

**Proposition 3.** *Let  $p_0$  be an umbilic point and  $\alpha(u, v) = (u, v, h(u, v))$  be as in equation (1).*

*If  $a = b = 0$  and  $cB \neq 0$  or if  $b = c = 0$  and  $aD \neq 0$ , then the principal configuration near  $p_0$  is as in Fig. 3.*

This umbilic point is denoted by  $D_{2h}^2$ .

*Proof.* Under these hypotheses, there are two singular points for the Lie-Cartan vector field 4; one is located at  $p = 0$  and the other at  $p = \infty$ , that is at  $q = 0$ .

Consider first the implicit differential equation of curvature lines

$$\begin{aligned} \mathcal{G}(u, v, q) &= -\frac{1}{2}Bu^2 + (k^3 - C)uv - \frac{1}{2}Dv^2 + O(3) \\ &+ [cv + \frac{1}{2}(C + 2k^3 - A)u^2 + (D - B)uv + \frac{1}{2}(E - 2k^3 - C)v^2 + O(3)]q \quad (7) \\ &+ [\frac{1}{2}Bu^2 - (k^3 - C)uv + \frac{1}{2}Dv^2 + O(3)]q^2 = 0. \end{aligned}$$

in the projective chart  $(u, v, q)$ , where  $q = du/dv$ . This implicit surface has a singularity of Morse type at  $(0, 0, 0)$  provided  $cB \neq 0$ . In such case, it has the topological structure of a cone.

In fact,

$$\text{Hess}(\mathcal{G})(0) = \begin{bmatrix} -B & k^3 - C & 0 \\ k^3 - C & -D & c \\ 0 & c & 0 \end{bmatrix}$$

Therefore,  $\det(\text{Hess}(\mathcal{G})(0)) = c^2 B \neq 0$ . The Lie-Cartan vector field

$$Y = (q\mathcal{G}_q, \mathcal{G}_q, -(\mathcal{G}_u q + \mathcal{G}_v))$$

is given by:

$$\begin{aligned} u' &= q[cv + \frac{1}{2}(C + 2k^3 - A)u^2 + (D - B)uv + \frac{1}{2}(E - 2k^3 - C)v^2 + O(3)] \\ v' &= cv + \frac{1}{2}(C + 2k^3 - A)u^2 + (D - B)uv + \frac{1}{2}(E - 2k^3 - C)v^2 + O(3) \\ q' &= (C - k^3)u + Dv - cq + \frac{1}{2}cu^2 + (c - 3k^2c)uv \\ &\quad + \frac{1}{2}a_{14}v^2 + (2B - D)uq + (2C - E + k^3)vq + O(3) \end{aligned}$$

Therefore,

$$DY(0) = \begin{bmatrix} 0 & 0 & 0 \\ 0 & c & 0 \\ C - k^3 & D & -c \end{bmatrix}$$

So, the nonzero eigenvalues of  $DY(0)$  are  $\lambda_1 = c$  and  $\lambda_2 = -c$  and 0 is a saddle point for  $Y_{\mathcal{G}}$ . The phase portrait of  $Y_{\mathcal{G}}$  is as shown in Fig. 7 below.

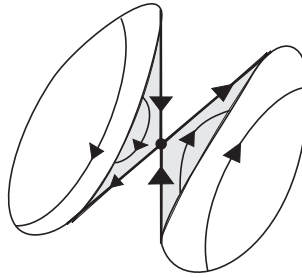


FIGURE 7. Cone at  $p = \infty$ ,  $q = 0$ .

Consider now the implicit differential equation

$$\begin{aligned}
\mathcal{F}(u, v, p) = & \left[ -\frac{1}{2}Bu^2 + (k^3 - C)uv - \frac{1}{2}Dv^2 - \frac{1}{6}a_{41}u^3 \right. \\
& - \frac{1}{2}a_{32}u^2v + \frac{1}{2}(3k^2c - a_{23})uv^2 - \frac{1}{6}a_{14}v^3 + O(4)]p^2 \\
& + [cv + \frac{1}{2}(C + 2k^3 - A)u^2 + (D - B)uv + \frac{1}{2}(E - 2k^3 - C)v^2 \\
& + \frac{1}{6}(a_{32} - a_{50})u^3 + \frac{1}{2}(2k^2c + a_{23} - a_{41})u^2v + \frac{1}{2}(a_{14} - a_{32})uv^2 \\
& + \frac{1}{6}(a_{05} - 6k^2c - a_{23})v^3 + O(4)]p \\
& + \frac{1}{2}Bu^2 - (k^3 - C)uv + \frac{1}{2}Dv^2 + \frac{1}{6}a_{41}u^3 \\
& + \frac{1}{2}a_{32}u^2v + \frac{1}{2}(a_{23} - k^2c)uv^2 + \frac{1}{6}a_{14}v^3 + O(4) = 0.
\end{aligned} \tag{8}$$

in the projective chart  $(u, v, p)$ , where  $p = dv/du$ .

This surface also has a singular point of Morse type at  $(0, 0, 0)$  with the topological structure of a cone, provided  $cB \neq 0$ .

As above, the Lie-Cartan vector field  $Z = (\mathcal{F}_p, p\mathcal{F}_p, -(\mathcal{F}_u + p\mathcal{F}_v))$  is given by:

$$\begin{aligned}
u' &= cv + \frac{1}{2}(C + 2k^3 - A)u^2 + (D - B)uv + \frac{1}{2}(E - 2k^3 - C)v^2 + O(3). \\
v' &= p[cv + \frac{1}{2}(C + 2k^3 - A)u^2 + (D - B)uv + \frac{1}{2}(E - 2k^3 - C)v^2 + O(3)] \\
p' &= -Bu + (k^3 - C)v - cp^2 + (A - k^3 - 2C)up + (B - 2D)vp \\
&\quad - \frac{1}{2}a_{41}u^2 - a_{32}uv + \frac{1}{2}(k^2c - a_{23})v^2 + O(3)
\end{aligned} \tag{9}$$

In this case the singular point  $(0, 0, 0)$  is not hyperbolic for the vector field  $Z = Z_{\mathcal{F}}$ . In fact,

$$DZ(0) = \begin{bmatrix} 0 & c & 0 \\ 0 & 0 & 0 \\ -B & k^3 - C & 0 \end{bmatrix},$$

and the three eigenvalues are zero.

In order to describe the phase portrait of  $Z$  near zero, observe that the sheets of the cone, with the origin removed, are located at  $p > 0$  and  $p < 0$ .

To describe the phase portrait of  $Z_{\mathcal{F}}$  near 0 it is suitable to perform the following weighted rescaling of variables.

$$u = r^2\bar{u}, \quad v = r^3\bar{v}, \quad p = r\bar{p}, \quad \bar{u}^2 + \bar{v}^2 + \bar{p}^2 = 1, \quad r \geq 0. \tag{10}$$

Then, from equation (8) it follows that

$$\begin{aligned}
 H(\bar{u}, \bar{v}, \bar{p}) &= \mathcal{F}(r^2\bar{u}, r^3\bar{v}, r\bar{p}) = c\bar{v}\bar{p} + \frac{1}{2}B\bar{u}^2 \\
 &\quad + r[(C - k^3)\bar{u}\bar{v} + \bar{u}^2\bar{p}(k^3 + \frac{1}{2}C)] + O(r^2) \quad (11)
 \end{aligned}$$

So, from equations (9) and (11), dropping the bars to simplify the notation and dividing by appropriate non negative functions, the following vector field is obtained:  $X = X_u \frac{\partial}{\partial u} + X_v \frac{\partial}{\partial v} + X_p \frac{\partial}{\partial p} + X_r \frac{\partial}{\partial r}$ , with

$$\begin{aligned}
 u' &= X_u = -2cv^2up + 3cv^3 + cp^2v + 2Bu^2p + 2cup^3 + rF_1(u, v, p, r) \\
 v' &= X_v = v(2cu^2p + 3Bup - 3cuv + 4cp^3) + rF_2(u, v, p, r) \\
 p' &= X_p = -cuvp - 2Bu^3 - 2cu^2p^2 - 3Buw^2 - 4cv^2p^2 + rF_3(u, v, p, r) \\
 r' &= X_r = r[cuv - Bup - cp^3 + cv^2p + rF_4(u, v, p, r)].
 \end{aligned}$$

In the expression above  $F_i(u, v, p, 0) = 0$ , ( $i = 1, \dots, 4$ ).

The restriction of  $X$  to the unitary sphere  $u^2 + v^2 + p^2 = 1$  is given by  $X_0 = X(u, v, p, 0)$  which has exactly six singular points, defined by the intersection of the curves

$$c_1(p) = (0, 0, p), \quad c_2(p) = \left(-\frac{cp^2}{B}, 0, p\right), \quad c_3(p) = \left(-\frac{4cp^2}{3B}, -\frac{8cp^3}{9B}, p\right)$$

with the unitary sphere.

A long, but straightforward, calculation leads to the following conclusions:

- i) The non zero eigenvalues of  $DX_0(c_1(p))$  are  $2cp^3$  and  $4cp^3$ .
- ii) The non zero eigenvalues of  $DX_0(c_2(p))$  are  $-2cp^3(2c^2p^2 + B^2)/B^2$  and  $cp^3(2c^2p^2 + B^2)/B^2$ .
- iii) The non zero eigenvalues of  $DX_0(c_3(p))$  are

$$-\frac{4}{81} \frac{cp^3}{B^2} (27B^2 + 96c^2p^2 + 64c^2p^4) \quad \text{and} \quad -\frac{2}{27} \frac{cp^3}{B^2} (27B^2 + 96c^2p^2 + 64c^2p^4).$$

Therefore, under the hypothesis  $cB \neq 0$ , the singular points at the curves  $c_1$  and  $c_3$  are hyperbolic (sinks and sources) and the singularities at  $c_2$  are hyperbolic saddles.

Also, the quadratic cone  $\mathcal{Q}_2(u, v, p) = cvp + \frac{B}{2}u^2 = 0$  is invariant by  $X_0$ ,  $\mathcal{Q}_2(c_1(p)) = \mathcal{Q}_2(c_3(p)) = 0$  and  $\mathcal{Q}_2(c_2(p)) \neq 0$ .

Summarizing, the phase portrait of  $X_0$  can be described as follows.

The intersection of the sphere with the cone  $\mathcal{Q}_2^{-1}(0)$  decomposes the sphere into two topological disks  $\bar{D}_1 \cup \bar{D}_2$  and one cylinder  $\bar{C}$ .

Each curve bounding the disks  $\bar{D}_1$  and  $\bar{D}_2$  is invariant by the flow of  $X_0$  and on it  $X_0$  has two hyperbolic singular points (one attractor and one repeller). Therefore in each disk the phase portrait of  $X_0$  has only one parallel canonical region. In the cylinder  $\bar{C}$ ,  $X_0$  has two hyperbolic saddles and the limit set of ordinary (i.e. non closed) orbits, perhaps with the

exception of the saddle separatrices, are the singularities contained in the bounding curves.

From the conclusions above, proceed to the analysis of the phase portrait of  $X$  in the coordinates  $(u, v, p, r)$ .

The four singular points on  $(c_1(p), 0)$  and  $(c_3(p), 0)$   $X$  are hyperbolic saddles of stability index 2 or 1; two of each type. In fact the normal derivatives of  $X$  in direction  $r$ , evaluated at the singularities above, are given by:

$$-cp^3, \quad \frac{1}{81} \frac{p^3 c(27B^2 + 64p^4 c^2 + 96c^2 p^2)}{B^2}.$$

The singular points  $(c_2(p), 0)$  are not hyperbolic for  $X$ , but for the purposes of our analysis it is not necessary to examine their topological type. The phase portrait of  $X$  at the conic critical point is illustrated in Fig. 8.

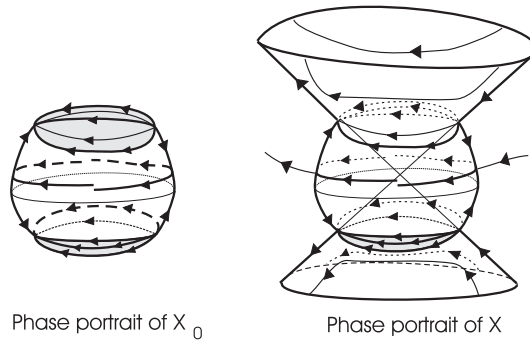


FIGURE 8. Blow up at the conic singular point for  $D_{2h}^2$

Therefore, near the projective line, the phase portrait of  $Z = Z_{\mathcal{F}}$ , restricted to the implicit surface  $\mathcal{F}^{-1}(0)$ , is as in Fig. 9. Here the point at  $\infty$  and that at 0 have been moved to finite conic points  $p_0$  and  $p_\infty$ , with  $p_0 p_\infty = -1$ , for better illustration.

Near the origin, the projective line is a center manifold with a quadratic semi-stable singularity. The other separatrix, asymptotic to the origin, sketched in Fig. 9, also behaves topologically as a semi-stable singularity. This is obtained by blowing down the phase portrait of  $X$  restricted to the cone.

Gluing together the phase portraits of  $Z = Z_{\mathcal{F}}$  near the projective line, in the charts  $(u, v, p)$  and  $(u, v, q)$ , ends the proof.  $\square$

#### 4. A SUMMARIZING THEOREM

A *bi-parametric family of immersed surfaces* will be a family  $\alpha_\lambda$  of immersions of an oriented surface  $\mathbb{M}$  into oriented  $\mathbb{R}^3$ , indexed by a parameter

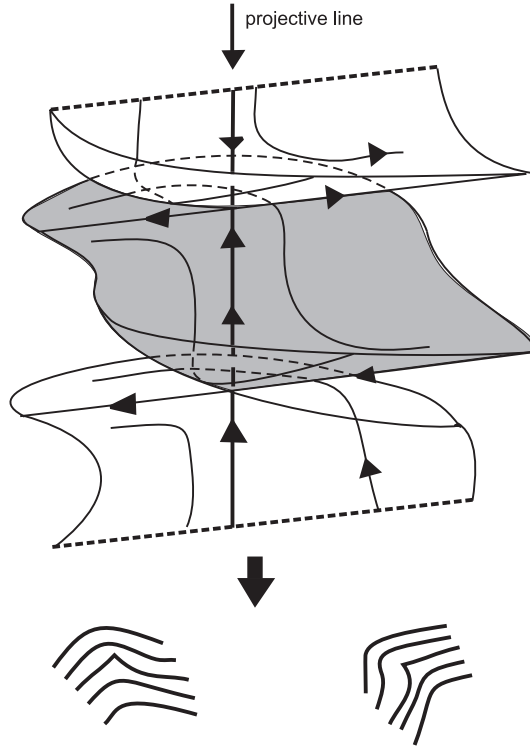


FIGURE 9. Lie-Cartan suspension of an umbilic point of type  $D_{2h}^2$

$\lambda$  ranging in another surface  $\mathbb{L}$ , of *parameters*. The families under consideration will be *smooth* in the sense that  $\alpha(m, \lambda) = \alpha_\lambda(m)$  is of class  $C^\infty$  in the product manifold  $\mathbb{M} \times \mathbb{L}$ . The space of families, denoted  $\mathcal{F}_{\mathbb{M} \times \mathbb{L}}$  will be endowed with the Whitney Fine Topology. See Levine [10] and Mather [12].

The term *generic*, referring to a property of families, means that it is valid for a collection of families which contains the intersection of countably many open dense sets in  $\mathcal{F}_{\mathbb{M} \times \mathbb{L}}$ . By the appropriate version of Baire Theorem, these collections are dense. See [10], [12], where can be found the basic terminology and concepts that are standard in Singularity Theory. Other reference on this subject, pertinent to geometric singularities, is Porteous [14].

For the sake of simplicity, from now on, the term *smooth* applied to mappings and manifolds will mean of *class*  $C^\infty$ . See [10, 12].

Consider the space  $\mathbb{J}^r(\mathbb{M}, \mathbb{R}^3)$  of  $r$ -jets of immersions,  $\alpha$ , of  $\mathbb{M}$  into  $\mathbb{R}^3$ , endowed with the structure of Principal Fiber Bundle. The base space is  $\mathbb{M} \times \mathbb{R}^3$ ; the fiber is the space  $\mathcal{J}^r(2, 3)$ , where  $\mathcal{J}^r(2, 3)$  is the space of  $r$ -jets of immersions of  $\mathbb{R}^2$  to  $\mathbb{R}^3$ , preserving the respective origins. The structure group,  $\mathbb{A}_+^r$ , is the product of the group  $\mathcal{L}_+^r(2, 2)$  of  $r$ -jets of origin

and orientation preserving diffeomorphisms of  $\mathbb{R}^2$ , acting on the right by coordinate changes, and the group  $\mathcal{O}_+(3, 3)$  of positive isometries; the action on the left consists on a positive rotation of  $\mathbb{R}^3$ .

Denote by  $\Pi_{r,s}$ ,  $r \leq s$  the projection of  $\mathcal{J}^s(2, 3)$  onto  $\mathcal{J}^r(2, 3)$ . It is well known that the group action comutes with projections, [10]. For the present needs, take  $r$  so that  $2 \leq r \leq 5$

Recall from Section 2 that each 5-jet of an immersion at an umbilic point is of the form  $(p, P, z)$ , with  $(p, P) \in \mathbb{M} \times \mathbb{R}^3$  and  $z$  is in the orbit of a polynomial immersion  $(u, v, h(u, v))$ , where

$$\begin{aligned} h(u, v) = & \frac{k}{2}(u^2 + v^2) + \frac{a}{6}u^3 + \frac{b}{2}uv^2 + \frac{c}{6}v^3 + \frac{A}{24}u^4 + \frac{B}{6}u^3v \\ & + \frac{C}{4}u^2v^2 + \frac{D}{6}uv^3 + \frac{E}{24}v^4 + \frac{a_{50}}{120}u^5 + \frac{a_{41}}{24}u^4v \\ & + \frac{a_{32}}{12}u^3v^2 + \frac{a_{23}}{12}u^2v^3 + \frac{a_{14}}{24}uv^4 + \frac{a_{05}}{120}v^5 \end{aligned} \quad (12)$$

Recall that the general quadratic part of  $h$  has the form  $\frac{k_{11}}{2}u^2 + k_{12}uv + \frac{k_{22}}{2}v^2$ . Therefore, the umbilic conditions  $k_{11} = k_{22}$ ,  $k_{12} = 0$ , imposed on jets, define a closed submanifold  $\mathcal{U}^5$ , of *umbilic jets*, of codimension 2 in  $\mathcal{J}^5(2, 3)$ .

Recall also that the general cubic part has also a term of the form  $\frac{b'}{2}u^2v$ . The expression in equation (12), is a representative of the orbit the an umbilic jets in the space  $(a, b, c)$ , with  $b' = 0$ .

Define below the *canonic umbilic stratification* of  $\mathcal{J}^5(2, 3)$ . The term *canonic* means that the strata are invariant under the action of the group  $\mathbb{A}_+^5 = \mathcal{O}_+(3, 3) \times \mathcal{L}_+^5(2, 2)$ . It is to the orbits of this action that reference is made below.

- 1) *Umbilic Jets*:  $\mathcal{U}^5$ , those in the orbits of  $j^5(u, v, h)$ , where  $h = h(u, v)$ , is as in equation (12), with  $k \in \mathbb{R}$ . It is a closed submanifold of codimension 2.
- 2) *Umbilic Jets with Rotationally Symmetric cubic part*:  $\mathcal{Q}^5$ , those in the orbit of  $j^5(u, v, h)$ , with  $h$  in expression (12) having  $a = b = b' = c = 0$ . It is a closed submanifold of codimension 4 inside  $\mathcal{U}^5$  and codimension 6 in  $\mathcal{J}^k(2, 3)$ .
- 3) *Non-Darbouxian Umbilic Jets*:  $(\mathcal{ND})^5$ , are those umbilic jets outside  $\mathcal{Q}^5$ , which are in the orbits of those whose expression (12) satisfy:

$$3.1) \tau = b(b - a) = 0 \text{ or}$$

$$3.2) b(b - a) \neq 0 \text{ and conditions } D_1 \text{ or } D_2 \text{ in Theorem 1 fail.}$$

$$\text{This is written } \delta_1 = a - 2b = 0 \text{ and } \delta = c^2 - 4b(a - 2b) = 0.$$

See Fig. 10 for an illustration of a spherical section the stratification of the intersection of  $(\mathcal{ND})^3$ , with the 3 space  $(a, b, c)$ , in the notation of equation (12).

The stratification on this sphere into points, curves and open sets, by the zeros of the homogeneous linear form  $\delta_1 = a - 2b$  and quadratic forms  $\tau = b(a - b)$  and  $\delta = c^2 - 4b(a - 2b) = 0$  and their complements is transferred



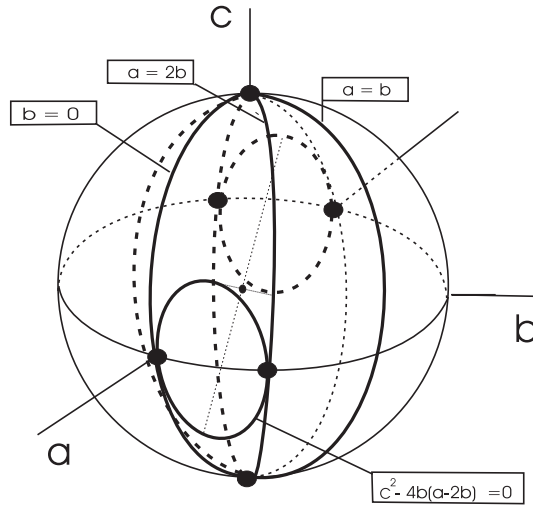


FIGURE 10. Stratification of a section of the fiber of  $(\mathcal{N}\mathcal{D})^3$ .

to  $(\mathcal{N}\mathcal{D})^5$  by the orbits of the group action, preserving the codimension of the strata inside  $\mathcal{U}^5$ . This codimension will be called *umbilic codimension*, to it 2 must be added to get the actual codimension inside  $\mathcal{J}^5(2, 3)$ .

4) The variety  $(\mathcal{N}\mathcal{D})^5$  of *Non-Darbouxian jets*, is further partitioned into

4.1)  $(\mathcal{D}_{2,3}^1)^5$ , defined by the orbits of jets with  $a = b \neq 0$ ,  $\chi \neq 0$ . See Theorem 2.

4.2)  $(\mathcal{D}_{2p}^2)^5$ , defined by the orbits of jets with  $a = b \neq 0$ ,  $\chi = 0$ ,  $b\xi < 0$ . See Proposition 2.

4.3)  $(\mathcal{D}_3^2)^5$ , defined by the orbits of jets with  $a = b \neq 0$ ,  $\chi = 0$ ,  $b\xi > 0$

4.4)  $(\mathcal{D}_{2h}^2)^5$ , defined by the orbits of jets with  $a = b = 0$ ,  $cB \neq 0$ . This is a manifold of umbilic codimension 2. See Proposition 3.

4.5)  $(\mathcal{D}_2^1)^5$  defined by the orbits of jets with  $c\tau \neq 0$  and  $\delta = 0$  or  $\delta_1 = 0$ . See Theorem 2. This is a manifold of umbilic codimension 1.

4.6)  $(\mathcal{D}_1^2)^5$  defined by the orbits of jets with  $c = 0$ ,  $b \neq 0$  and  $\delta_1 = 0$ . See Proposition 1. This is a manifold of umbilic codimension 2.

4.7)  $\mathcal{Z}^5$ , defined by the orbits of jets with  $a = b \neq 0$ ,  $\chi = 0$ ,  $\xi = 0$ , which is a subvariety of umbilic codimension 3.

4.8)  $\mathcal{W}^5$ , defined by the orbits of jets with  $a = b \neq 0$ ,  $B = 0$ , which is a subvariety of umbilic codimension 3.

5) The orbits passing through the open sets in Fig. 10 correspond to the Darbouxian umbilic jets:  $(\mathcal{D}_i)^5$ ,  $i = 1, 2, 3$ .

The *canonic stratification* of  $\mathcal{J}^5(2, 3)$  induces a canonic stratification of  $\mathbb{J}^5(\mathbb{M}, \mathbb{R}^3)$  whose strata are principal sub-bundles, with codimension equal to that of their fibers, which are the canonic strata of  $\mathcal{J}^5(2, 3)$ , as defined above in items 1, 2, 3, 4 and 5.

The collection of sub-bundles which stratify  $\mathbb{J}^5(\mathbb{M}, \mathbb{R}^3)$  will be called *umbilic stratification*. The strata are:  $\mathbb{U}^5(\mathbb{M}, \mathbb{R}^3)$ , corresponding to  $\mathcal{U}^5$ ;  $\mathbb{D}^5_i(\mathbb{M}, \mathbb{R}^3)$ ,  $i = 1, 2, 3$ , corresponding to the strata of Darbouxian umbilic jets  $(\mathcal{D}_i)^5$ ,  $i = 1, 2, 3$ , and so on, one bundle for each of the strata in the items above.

**Theorem 3.** The following properties are generic for smooth bi-parametric families,  $\alpha_\lambda$ , of immersions in  $\overline{\mathcal{F}}_{\mathbb{M} \times \mathbb{L}}$ .

The set  $\mathbb{U}(\alpha_\lambda)$  to  $\mathbb{L}$  points  $(m, \lambda)$  in  $\mathbb{M} \times \mathbb{L}$  such that  $m$  is an umbilic point of  $\alpha_\lambda$  form a smooth regular surface, which is stratified as follows:

Darbouxian umbilics,  $D_1$ ,  $D_2$  and  $D_3$ , occur on regular surfaces,

Codimension one umbilics,  $D_2^1$  and  $D_{2,3}^1$ , occur along regular curves,

Codimension two umbilics,  $D_1^2$ ,  $D_{2p}^2$ ,  $D_3^2$  and  $D_{2h}^2$ , occur at isolated points.

*Proof.* Apply Thom Transversality Theorem in Jet Spaces, to make the jet extension  $j^5\alpha_\lambda$ , as a mapping of  $\mathbb{M} \times \mathbb{L}$ , transversal to the canonic stratification of  $\mathbb{J}^5(\mathbb{M}, \mathbb{R}^3)$ . See Levine [10] and Mather [12].

Notice that the strata not listed in the statement of the Theorem have codimensions larger than 4 and therefore are avoided by transversality. While the other strata, listed there, give the right structure of regular surfaces, curves and points claimed in the Theorem, since they are obtained by the pull back of the canonic strata by a  $j^5\alpha_\lambda$  transversal to them. □

**Remark 2.** In [5], the curves and points above in Theorem 3 will be better organized in terms of Whitney folds and cusps of the projection of  $\mathbb{U}(\alpha_\lambda)$  to  $\mathbb{L}$ . See [10].

## REFERENCES

- [1] A. ANDRONOV, E. LEONTOVICH ET AL, Theory of Bifurcations of Dynamic Systems on a Plane, Jerusalem , Israel Program of Scientific Translations, 1973.
- [2] B. BRUCE and D. FIDAL, *On binary differential equations and umbilic points*, Proc. Royal Soc. Edinburgh **111A**, (1989), pp. 147-168.
- [3] G. DARBOUX, *Leçons sur la Théorie des Surfaces*, vol. IV. Sur la forme des lignes de courbure dans la voisinage d'un ombilic, Note 07, Paris:Gauthier Villars, 1896.
- [4] R. GARCIA, C. GUTIERREZ and J.SOTOMAYOR; *Bifurcations of Umbilical Points and Related Principal Cycles*, Jour. Dyn. and Diff. Equations, **16**, (2004), pp. 321-346.
- [5] R. GARCIA and J.SOTOMAYOR, *Bifurcations of Codimension two Umbilic Points*, In preparation.
- [6] C. GUTIERREZ and V. GUINEZ, Rank-1 codimension one of positive quadratic differential forms, J. of Differential Equations **206** , (2004), pp. 127-155.
- [7] C. GUTIERREZ and J. SOTOMAYOR, Structural Stable Configurations of Lines of Principal Curvature, Asterisque **98-99**, (1982), pp. 185-215.
- [8] C. GUTIERREZ and J. SOTOMAYOR, Lines of Curvature and Umbilic Points on Surfaces, 18<sup>th</sup> Brazilian Math. Colloquium, Rio de Janeiro, IMPA, 1991. Reprinted with

- update as Structurally Configurations of Lines of Curvature and Umbilic Points on Surfaces, Lima, Monografias del IMCA, 1998.
- [9] C. GUTIERREZ and J. SOTOMAYOR, *Lines of Curvature and Bifurcations of Umbilical Points*, Colloquium on dynamical systems (Guanajuato, 1983), pp. 115–126, Aportaciones Mat. **05**, Soc. Mat. Mexicana, México, 1985.
  - [10] H.T. LEVINE, Singularities of Differentiable Mappings, Lect. Notes in Math. **192**, (1971), pp. 1–89.
  - [11] S. LOPEZ DE MEDRANO, *A splitting lemma for  $C^r$  functions*,  $r \geq 2$ , Singularity theory (Trieste, 1991), 444–450, World Sci. Publishing, River Edge, NJ, 1995.
  - [12] J. MATHER; *Stability of  $C^\infty$  mappings*, *V : Transversality*, Advances in Math. **04**, 3, (1970), pp. 301–336.
  - [13] G. MONGE Sur les lignes de Courbure de la surface de l'ellipsoïde, Journ. Ecole Polytech., II cah. 1796.
  - [14] I. PORTEOUS, Geometric Differentiation, Cambridge Univ. Press, 1994.
  - [15] J. SOTOMAYOR, Historical Comments on Monge's Ellipsoid and the Configuration of Lines of Curvature on Surfaces Immersed in  $\mathbb{R}^3$ , Mathematics ArXiv, <http://front.math.ucdavis.edu/math.HO/0411403>.
  - [16] M. SPIVAK, Introduction to Comprehensive Differential Geometry, Vol. III, Publish or Perish, Inc., Wilmington, Del., 1979.
  - [17] D. STRUIK, Lectures on Classical Differential Geometry, Addison Wesley Pub. Co., Reprinted by Dover Publications, Inc., 1988.
  - [18] R. THOM, Stabilité Structurale et Morphogénèse, W. A. Benjamin, Inc., 1972.

Jorge Sotomayor  
Instituto de Matemática e Estatística,  
Universidade de São Paulo,  
Rua do Matão 1010, Cidade Universitária,  
CEP 05508-090, São Paulo, S.P., Brazil

Ronaldo Garcia  
Instituto de Matemática e Estatística,  
Universidade Federal de Goiás,  
CEP 74001-970, Caixa Postal 131,  
Goiânia, GO, Brazil